Journal of Organometallic Chemistry, 310 (1986) 317–332
Elsevier Sequoia S.A., Lausanne – Printed in The Netherlands

CYCLIC SILYLAMIDES OF VANADIUM, NIOBIUM, TANTALUM AND HAFNIUM. CRYSTAL AND MOLECULAR STRUCTURES OF SPIROCYCLIC TETRAAMIDES OF V^{IV}, CH_3Nb^{V} AND Hf^{IV}

D.J. BRAUER, H. BÜRGER, G.R. LIEWALD and J. WILKE

Anorganische Chemie, Fachbereich 9, Universität-Gesamthochschule, D-5600 Wuppertal (F.R.G.)

(Received February 25th, 1986)

Summary

The spirocyclic silylamides $M[(NR)_2SiMe_2]_2$ (R = t-Bu: M = Hf (III), V (IV); R = $SiMe_3$: M = V (V), NbCl (VI), TaCl (VII)) have been prepared by reaction of the $HfCl_4$, VCl_4, $NbCl_5$ and $TaCl_5$, respectively, with $Me_2Si[N(Li)R]_2$. Methylation of VI and VII with MeLi yields the respective $NbCH_3$ and $TaCH_3$ derivatives (VIII and IX). The effective magnetic moments of IV and V are 1.67 and 1.66 μ_B respectively. Infrared and Raman spectra are given, and the ^1H, ^{13}C and ^{29}Si chemical shifts for the diamagnetic compounds are reported. Single-crystal X-ray studies have been performed on III, IV and VIII. The structures of III and IV possess distorted tetrahedral symmetry (D_{2d}), with mean M–N distances of 2.030(4) and 1.853(5) Å, respectively. Distorted trigonal-bipyramidal coordination with an equatorial methyl group is found for each Nb atom of the two crystallographically independent molecules of VIII. Mean Nb–C, Nb–N (equatorial) and Nb–N (axial) bond lengths are 2.218(9), 1.997(4) and 2.026(5) Å, respectively.

Introduction

Although disilylamides of the Group IVA and VA transition metal elements Ti, Zr and V were synthesized in the sixties and were among the first fully characterized transition metal silylamides [1], the analogous derivatives of Hf [2] and Ta [3] were not described until 1979. Niobium disilylamides have not yet been reported. At most three $N(SiR_3)_2$ groups have been attached to the transition metal atoms, the steric demands of these groups preventing their attachment at the fourth or fifth coordination site.

On the other hand, the bidentate groups $X(NR')_2$ ($X = Me_2Si$, $Me_2SiSiMe_2$), $Me_2SiZSiMe_2$ ($Z = CH_2$, O, NR), which also are disilylamido ligands when R = $SiMe_3$, can occupy up to four coordination sites of the early transition metal atoms. Comparison of spirocyclic Ti and Zr derivatives, R' = alkyl or $SiMe_3$, of various ring

0022-328X/86/$03.50

sizes reveals that the four-membered ring species **C** are thermally and chemically more stable than the six- and five-membered ring species **A** and **B**.

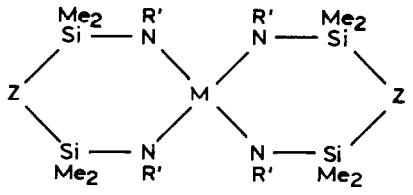

A

(M = Ti[4] ; Zr[5])

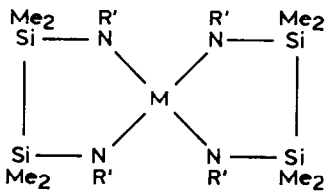

B

(M = Ti[6] ; Zr[7])

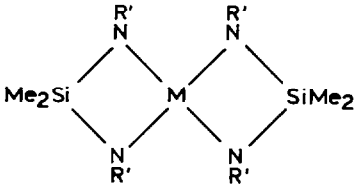

C

(M = Ti[8] ; Zr[9])

Furthermore, the known derivatives of type **C**, R′ = t-Bu and $SiMe_3$, are crystalline solids sufficiently volatile to be sublimed in vacuo without decomposition. Therefore attempts to synthesize derivatives of the Group VA elements V, Nb and Ta and to determine their crystal and molecular structures seemed promising. A previous investigation dealt with type **A** amides of V^{IV}, R′ = Me, Z = NMe and CH_2 [10]; despite the pronounced instability of these compounds, they were fully characterized.

While type **C** derivatives with R′ = $SiMe_3$ are transition metal disilylamides, the corresponding R′ = t-Bu analogues are silylalkylamides. Both types of species have been reported for M = Ti [8] and Zr [9,11], but only the $SiMe_3$ derivative has been made for M = Hf [11]. In order to permit a well-based comparison of analogous t-Bu and $SiMe_3$ spiranes, we attempted to synthesize the missing t-Bu derivate of M = Hf and to obtain both the t-Bu and $SiMe_3$ derivatives of the Group VA elements. In the present study we report on our attempts to synthesize the first tetraamides of Group VA elements with spirobicycloheptane structure, and describe the crystal and molecular structures of spirocycles with M = Hf, V and CH_3Nb as spiro centers.

Synthesis

The type **C** spirocyclic amides with M = Hf, R = t-Bu (III); M = V, R = t-Bu (IV); M = V, R = $SiMe_3$ (V); M = NbCl, R = $SiMe_3$ (VI); M = TaCl, R = $SiMe_3$ (VII) were obtained by the reaction of the dilithiated silylamines $Me_2Si[N(Li)\text{-}t\text{-}Bu]_2$ (I) and $Me_2Si[N(Li)SiMe_3]_2$ (II) with the respective halides $HfCl_4$, VCl_4, $NbCl_5$ and $TaCl_5$, in yields ranging from 23 (VII) to 53% (V), eq. 1.

$$2\ \mathrm{I, II} + MCl_4 \rightarrow 4\ LiCl + \mathbf{C} \qquad (1)$$

All the compounds have been isolated by sublimation in vacuo. Attempts to obtain pure material by crystallization were not successful; the reluctance of the compounds to crystallize out from the reaction mixture is probably also responsible for the failure to isolate defined products from the reaction of VCl_4 with dilithiated $Ph_2Si(NHSiMe_3)_2$ and of $NbCl_5$ and $TaCl_5$ with I. Though the reactions seemed to proceed reasonably well, as judged from the quantity of LiCl formed, the products decomposed when sublimation was tried.

Alkylation of [bis(trimethylsilyl)amido]-hafnium [2,12] and tantalum chlorides [3] has been described previously. In order to assess the reactivity of the M-Cl group in VI and VII, methylation with MeLi was attempted; the methyl derivatives VIII and IX were obtained in yields of 82 and 65%, respectively.

Properties

The physical properties of III to IX are set out in Table 1. The paramagnetic V^{IV} compounds are deeply coloured and the Nb^V derivatives VI and VIII are yellow, but the Hf and Ta amides are colourless. All the compounds can be sublimed in vacuo, only VIII showing any decomposition. Owing to the deep colour of V its melting point and decomposition temperature could not be determined visually, and no exothermic or endothermic peaks were detected by differential thermal analysis. All the compounds are readily soluble in aliphatic and aromatic hydrocarbons and ether, and are stable in absence of air. Compounds III and V are particularly sensitive, whereas IV decomposes only slowly in moist air. Compounds IV and V are paramagnetic, and the effective magnetic moments determined by the NMR method [13] are 1.67 and 1.66 μ_B, values consistent with those for type A amides of vanadium(IV) [10].

TABLE 1

PHYSICAL PROPERTIES AND NMR SPECTRA OF COMPOUNDS III TO IX

	III	IV	V	VI	VII	VIII	IX
M.p. (°C)	172–174	>155 (dec.)	[a]	126–129	131–133	~102 (dec.)	137–139
Subl. temp. (°C) /10^{-3} Torr	70	70	70	100	100	80 (dec.)	90
Colour	colourless	red	dark-green	yellow	colourless	yellow	colourless
δ(¹H) (ppm) [b]							
CMe_3, $SiMe_3$	1.25			0.20	0.19	0.16	0.15
$SiMe_2$	0.35			0.47	0.46	0.39	0.40
MCH_3						0.76	0.53
δ(¹³C) (ppm) [c]							
$Si(CH_3)_3$, $C(CH_3)_3$	36.70			3.26	3.63	3.90	4.15
$Si(CH_3)_2$	6.20			4.68	4.76	5.36	5.40
$C(CH_3)_3$	56.03						
MCH_3						[a]	42.80
δ(²⁹Si) (ppm) [d]							
$SiMe_3$				3.68	3.44	0.81	1.06
$SiMe_2$	−41.24			−34.17	−35.87	−33.80	−34.27

[a] See text. [b] In CCl_4 against internal TMS. [c] In C_6D_6 127.96 ppm. [d] In C_6D_6 against external TMS.

Oxidation of IV and V should yield diamagnetic species, and therefore ^1H NMR should be well suited for following this process. Use of stoichiometric amounts of Cl_2 and I_2 in CCl_4 or CH_2Cl_2 did not yield any diamagnetic species, but a series of diamagnetic products was formed with Br_2; no individual compound could be isolated from the product mixtures by crystallization or sublimation in vacuo. The halogen may have cleaved Si–N bonds rather than directly oxidizing the sterically shielded V atom. In order to obtain more insight into the possible oxidation, solutions of IV and V in $CH_3CN/0.1\ M\ Et_4NClO_4$ were studied cyclovoltammetrically between +1000 and −1000 mV; Cp_2Fe/Cp_2Fe^+ +92 mV ($E°$ +350 mV vs. SCE) was used as reference. Compound V turned out to be electrochemically inert in the investigated region, but the cyclovoltagram of IV exhibited irreversible oxidation peaks at −355 and +750 mV relative to Cp_2Fe. The first peak is probably due to a cation IV^+ which rapidly decomposes to the species responsible for the second.

Attempts to reduce VI and VII to Nb^{IV} and Ta^{IV} species analogous to V were also fruitless. There was no reaction with Li, Na or Zn in nonpolar solvents, but Li in THF and sodium amalgam caused breakdown of the spirocyclic framework. Complex hydrides, e.g. $LiBH_4$, $NaBH_4$ and $LiAlH_4$, which have been shown to form complex hydrides with chlorodisilylamides of Th, U [14], Zr and Hf [12], did not react with VI and VII.

Spectra

NMR spectra

The ^1H, ^{13}C and ^{29}Si NMR spectra of III, VI, VII, VIII and IX are listed in Table 1. The ^{13}C signal of the $NbCH_3$ group in VIII was not detected, possibly because of incomplete relaxation of the ^{93}Nb nucleus ($I = 9/2$). The ^{13}C signal of the $TaCH_3$ group in IX, at δ 42.8 ppm, appears at higher field than that in $(CH_3)_3Ta[N(SiMe_3)_2]_2$, $\delta = 65.0/56.5$ ppm [3]. No NMR spectra of the paramagnetic species IV and V were obtained.

Vibrational spectra

Infrared and Raman spectra of the compounds were recorded, except for the Raman spectrum of V which is too deeply coloured. The spectra are listed in the Experimental section. The spectra of analogous molecules (III/IV, VI/VII and VIII/IX) are almost identical. In addition to the typical group vibrations of the ligands, some vibrations attributable to the spirane frame have been assigned. The intense Raman line in III and IV near 540 cm^{-1}, which is without an infrared counterpart, is assigned to the symmetric MN_4 stretching vibration. Vibrations associated with the $Si(NSi)_2M$ skeleton and denominated ω_1, ω_1', ω_4, ω_5 and ω_6 [15] were observed as follows (cm^{-1}):

	V	VI	VII	VIII	IX
ω_1 (IR)	996	950	955	955	955
ω_1' (Ra)	–	1029	1046	1036	1043
ω_4 (IR, Ra)	–	434	440	435	438
ω_5 (Ra)		362	363	351	353
ω_6 (IR)	403	401	397	405	395

Of the vibrations of the MCH_3 unit, $\delta_s(CH_3)$ may be assigned to Raman lines at 1151 and 1171 cm^{-1}, while $\nu(MC)$ is tentatively attributed to Raman lines at 482 and 489 cm^{-1}, for VIII and IX respectively.

Mass spectra

Low resolution EI mass spectra of III to IX were obtained. The isotopic effect of Hf and Cl gives rise to characteristic patterns. Peaks of molecular ions M^+ are weak for III and IV, but M^+ is the base peak for V. In VI to IX, the $(M - CH_3)^+$ peak is the highest mass peak observed. Lists of peaks are given in the Experimental section. Since the paramagnetic species IV and V could not be investigated by NMR spectroscopy, their M^+ molecular ion mass peaks were measured under high resolution conditions. IV: $^{12}C_{20}\ ^{1}H_{48}\ ^{14}N_4\ ^{28}Si_2\ ^{51}V\ M^+$ calculated 451.2857, observed 451.2856. V: $^{12}C_{16}\ ^{1}H_{48}\ ^{14}N_4\ ^{28}Si_6\ ^{51}V\ M^+$ calculated 515.1935, observed 515.1930.

Electronic spectra

The UV/VIS spectra of IV and V in n-hexane are dominated by the intense N → V CT absorptions at 30800/22200 and 32000/24000 cm^{-1}, respectively. While for IV the *d–d* transitions are evidently hidden under the strong CT absorptions, in the case of V two maxima, at 17700 cm^{-1} (ϵ 150 l mol^{-1} cm^{-1}) and 16390 cm^{-1} (ϵ 100 l mol^{-1} cm^{-1}), are well pronounced. In agreement with previous assignments for type **A** spiranes and data for $V(NR'_2)_4$ complexes [15], these maxima are tentatively attributed to $d_{x^2-y^2} \rightarrow d_{xz}$, d_{yz} and $d_{z^2} \rightarrow d_{xz}$, d_{yz} transitions of a Jahn-Teller distorted VN_4 tetrahedron with a splitting of the (T_d) into b_1 ($d_{x^2-y^2}$) and $a_1(d_{z^2})$ levels for D_{2d} symmetry.

X-Ray structure determinations

Crystals of III, IV and VIII were sealed in thin-walled glass capillaries under argon. Intensity data on III and VIII were collected in the usual manner [18] with a Siemens AED 1 diffractometer employing Zr-filtered, Mo-$K_{\bar{\alpha}}$ (0.71073 Å) radiation. Data on IV were obtained as described previously with an Enraf–Nonius CAD-4 diffractometer using Ni-filtered Cu-$K_{\bar{\alpha}}$ (1.54178 Å) X-rays [19]. The data were corrected for fluctuations of the monitor reflections and for absorption.

The structures were solved by heavy atom techniques and refined by full-matrix (III, IV) or large-block least-squares methods (VIII). Only data with $|F_o| \geqq 4\sigma(|F_o|)$ were used in the refinement. Dispersion-corrected scattering factors were taken from the usual tables [20]. Since the positions of the hydrogen atoms of the $NbCH_3$ groups could not be derived from difference Fourier maps calculated in the final stages of refinement, these atoms were not introduced into the model. All other hydrogen atoms were placed in ideal positions (C–H 0.95 Å, H–C–H 109.5°, staggered), allowed to ride on the corresponding carbon atom, and assigned group isotropic thermal parameters. Anisotropic refinement of the other atoms converged in each case, and the final difference Fourier syntheses contained no chemically significant features.

Crystal data and details of the refinement are given in Table 2. Positional parameters of the nonhydrogen atoms are presented in Tables 3, 4 and 5, and the

(Continued on p. 325)

TABLE 2

CRYSTAL DATA

	$Hf[(N\text{-}t\text{-}Bu)_2SiMe_2]_2$	$V[(N\text{-}t\text{-}Bu)_2SiMe_2]_2$	$MeNb[(NSiMe_3)_2SiMe_2]_2$
M_r	579.29	451.74	573.039
Crystal system	monoclinic	tetragonal	monoclinic
Reflection conditions	hkl, $h+k=2n$ $h0l$, $l(h)=2n$	hkl, $h+k+l=2n$ $h0l$, $h(l)=2n$ $0k0$, $k=4n$	$h0l$, $h=2n$ $0k0$, $k=2n$
Space group	$C2/c$	$I4_1/a$	$P2_1/a$
T (°C)	31	21	22
a (Å)	18.906(3)	18.590(3)	18.029(7)
b (Å)	8.921(2)	18.590(3)	18.905(7)
c (Å)	21.114(3)	33.212(3)	21.369(5)
β (°)	124.471(9)	90	114.64(2)
Z	4	16	8
D_x (g cm^{-3})	1.310	1.046	1.150
2θ-limits (°)	4–50	2–120	4–45
Monitor correction	1.000–0.875	1.000–1.083	0.999–1.064
Crystal size (mm)	0.20×0.36×0.41	0.10×0.38×0.38	0.14×0.30×1.08
μ (cm^{-1})	36.1	38.1	5.68
Transmission	0.318–0.502	0.316–0.691	0.836–0.921
Unique reflections	2592	4244	8617
Observed ($F \geqq 4\sigma(F)$)	2099	1941	5721
Parameters	131	260	521
$\lvert\xi/\sigma\rvert_{max}$	0.25	0.03	0.35
P	0.0009	0.0004	0.0009
R^a	0.046	0.055	0.067
R_w^a	0.056	0.048	0.086
Final $\Delta\rho$ (e/Å^3)	1.18 to −0.74	0.27 to −0.26	1.14 to −1.38

[a] $R = \Sigma\Delta/\Sigma|F_o|$ and $R_w = [\Sigma w\Delta^2/\Sigma w|F_o|^2]^{1/2}$ where $w = (\sigma^2(|F_o|) + p|F_o|^2)^{-1}$ and $\Delta = ||F_o| - |F_o||$, summations being taken over the observed reflections only.

TABLE 3

POSITIONAL AND EQUIVALENT ISOTROPIC TEMPERATURE FACTORS [a] FOR $Hf[(N\text{-}t\text{-}Bu)_2SiMe_2]_2$

Atom	x	y	z	U
Hf	0.0000	0.19474(5)	0.2500	0.0570(2)
Si	−0.0023(1)	0.1856(3)	0.3791(1)	0.073(1)
N(1)	−0.0594(4)	0.2929(7)	0.2945(4)	0.063(3)
N(2)	0.0594(4)	0.0919(8)	0.3539(3)	0.064(3)
C(1)	0.0613(8)	0.297(2)	0.4687(6)	0.118(7)
C(2)	−0.0729(8)	0.055(2)	0.3887(7)	0.122(8)
C(3)	−0.1253(6)	0.409(1)	0.2721(6)	0.084(6)
C(4)	−0.157(1)	0.461(2)	0.196(1)	0.21(2)
C(5)	−0.194(1)	0.353(2)	0.276(2)	0.25(3)
C(6)	−0.091(1)	0.536(2)	0.321(1)	0.28(2)
C(7)	0.1251(6)	−0.026(1)	0.3959(5)	0.084(5)
C(8)	0.162(1)	−0.064(3)	0.354(1)	0.23(2)
C(9)	0.195(1)	0.029(2)	0.4725(9)	0.25(1)
C(10)	0.091(1)	−0.159(2)	0.408(1)	0.21(2)

[a] $U = \frac{1}{3}\Sigma_i\Sigma_j U_{ij} a_i^* a_j^* \bar{a}_i \cdot \bar{a}_j$.

TABLE 4

POSITIONAL AND EQUIVALENT ISOTROPIC TEMPERATURE FACTORS [a] FOR V[(N-t-Bu)$_2$SiMe$_2$]$_2$

Atom	x	y	z	U
V	0.06832(5)	−0.00519(5)	0.24669(3)	0.0432(4)
Si(1)	0.0520(1)	−0.0600(1)	0.31742(6)	0.0645(8)
Si(2)	0.0815(1)	0.0493(1)	0.17558(5)	0.0655(8)
N(1)	0.0052(3)	0.0033(3)	0.2891(1)	0.053(2)
N(2)	0.1150(2)	−0.0716(2)	0.2793(1)	0.054(2)
N(3)	0.1117(2)	0.0745(2)	0.2229(1)	0.047(2)
N(4)	0.0393(2)	−0.0273(2)	0.1948(1)	0.057(2)
C(1)	−0.0004(4)	−0.1427(3)	0.3298(2)	0.094(3)
C(2)	0.0883(4)	−0.0249(4)	0.3660(2)	0.121(4)
C(3)	−0.0593(4)	0.0458(5)	0.2983(3)	0.087(4)
C(4)	−0.0865(4)	0.0814(5)	0.2604(3)	0.148(5)
C(5)	−0.1175(4)	0.0009(5)	0.3158(3)	0.172(6)
C(6)	−0.0412(6)	0.1048(6)	0.3272(4)	0.223(8)
C(7)	0.1785(4)	−0.1165(4)	0.2766(3)	0.089(4)
C(8)	0.2157(4)	−0.1064(5)	0.2377(3)	0.164(6)
C(9)	0.1577(6)	−0.1941(6)	0.2801(4)	0.242(9)
C(10)	0.2309(6)	−0.1023(8)	0.3094(4)	0.26(1)
C(11)	0.0193(4)	0.1164(4)	0.1513(2)	0.123(4)
C(12)	0.1549(4)	0.0295(4)	0.1385(2)	0.110(4)
C(13)	0.1517(4)	0.1379(4)	0.2361(2)	0.063(3)
C(14)	0.1796(6)	0.1261(5)	0.2779(3)	0.174(6)
C(15)	0.2143(4)	0.1532(4)	0.2087(2)	0.117(4)
C(16)	0.1044(5)	0.2035(4)	0.2357(3)	0.170(6)
C(17)	−0.0033(5)	−0.0848(4)	0.1750(2)	0.086(4)
C(18)	−0.0346(5)	−0.1330(4)	0.2062(3)	0.138(5)
C(19)	−0.0659(6)	−0.0516(5)	0.1525(3)	0.197(7)
C(20)	0.0413(6)	−0.1266(6)	0.1466(3)	0.206(7)

[a] See Table 3.

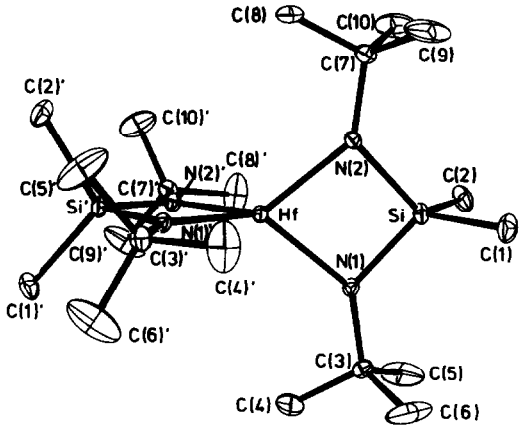

Fig. 1. A perspective drawing of Hf[(N-t-Bu)$_2$SiMe$_2$]$_2$ with 5% probability thermal ellipsoids and H atoms omitted.

TABLE 5

POSITIONAL AND EQUIVALENT ISOTROPIC THERMAL [a] PARAMETERS FOR $MeNb[(NSiMe_3)_2SiMe_2]_2$

Atom	x	y	z	U	Atom	x	y	z	U
Nb(1)	0.04296(5)	0.24490(4)	0.88280(4)	0.0421(3)	Nb(2)	0.32934(5)	0.26789(4)	0.37840(4)	0.0436(3)
Si(11)	0.0432(2)	0.3609(1)	0.9591(1)	0.053(1)	Si(21)	0.4172(2)	0.1595(1)	0.4616(1)	0.060(1)
Si(12)	0.0107(2)	0.2299(1)	1.0311(1)	0.064(1)	Si(22)	0.5070(2)	0.3001(2)	0.5229(1)	0.073(1)
Si(13)	0.0615(2)	0.4199(1)	0.8316(1)	0.066(1)	Si(23)	0.2812(2)	0.0885(1)	0.3350(2)	0.085(2)
Si(14)	−0.0295(2)	0.1209(1)	0.8244(1)	0.062(1)	Si(24)	0.3239(2)	0.3914(1)	0.3116(1)	0.056(1)
Si(15)	−0.1521(2)	0.2419(2)	0.7480(1)	0.068(1)	Si(25)	0.3900(2)	0.2759(2)	0.2433(1)	0.066(1)
Si(16)	0.1485(2)	0.0831(1)	0.9273(2)	0.067(1)	Si(26)	0.2514(2)	0.4242(1)	0.4172(1)	0.063(1)
N(11)	0.0436(4)	0.2703(3)	0.9739(3)	0.053(3)	N(21)	0.4229(4)	0.2514(4)	0.4697(3)	0.057(3)
N(12)	0.0416(4)	0.3527(3)	0.8779(3)	0.047(3)	N(22)	0.3378(5)	0.1609(3)	0.3796(3)	0.060(4)
N(13)	−0.0606(4)	0.2099(4)	0.8085(3)	0.052(3)	N(23)	0.3515(5)	0.3052(3)	0.3006(3)	0.055(3)
N(14)	0.0662(4)	0.1399(3)	0.8911(4)	0.050(3)	N(24)	0.3023(4)	0.3710(3)	0.3815(3)	0.047(3)
C(11)	0.1532(7)	0.2525(5)	0.8611(7)	0.092(6)	C(21)	0.2003(6)	0.2486(5)	0.3575(7)	0.089(6)
C(12)	−0.0492(7)	0.4058(5)	0.9587(5)	0.084(6)	C(22)	0.5134(7)	0.1186(6)	0.4658(6)	0.102(7)
C(13)	0.1369(6)	0.4051(5)	1.0216(5)	0.078(5)	C(23)	0.3899(7)	0.1161(6)	0.5259(5)	0.088(6)
C(14)	0.0457(9)	0.2835(6)	1.1116(5)	0.107(8)	C(24)	0.4772(8)	0.3911(6)	0.5383(7)	0.118(7)
C(15)	−0.0994(8)	0.2216(7)	0.9932(7)	0.109(8)	C(25)	0.5816(8)	0.3073(7)	0.4835(8)	0.128(9)
C(16)	0.0555(8)	0.1409(5)	1.0569(6)	0.093(6)	C(26)	0.555(1)	0.2570(8)	0.6091(6)	0.164(9)
C(17)	0.0259(7)	0.3944(6)	0.7402(5)	0.095(7)	C(27)	0.353(1)	0.0158(7)	0.3368(8)	0.15(1)
C(18)	0.0072(8)	0.5011(5)	0.8364(6)	0.106(7)	C(28)	0.2133(9)	0.0551(7)	0.3703(7)	0.140(9)
C(19)	0.1729(7)	0.4427(6)	0.8652(6)	0.100(7)	C(29)	0.220(1)	0.1124(7)	0.2435(6)	0.16(1)
C(110)	−0.0942(6)	0.0668(6)	0.8530(7)	0.100(7)	C(210)	0.2327(7)	0.4234(5)	0.2362(5)	0.091(6)
C(111)	−0.0214(7)	0.0786(6)	0.7494(6)	0.118(7)	C(211)	0.4096(7)	0.4558(6)	0.3342(6)	0.093(7)
C(112)	−0.2360(7)	0.1798(8)	0.7405(7)	0.138(9)	C(212)	0.460(1)	0.3426(8)	0.2339(9)	0.15(1)
C(113)	−0.1755(8)	0.3285(7)	0.7740(7)	0.139(8)	C(213)	0.4487(9)	0.1939(7)	0.2731(7)	0.128(9)
C(114)	−0.1519(9)	0.2480(8)	0.6628(5)	0.132(8)	C(214)	0.307(1)	0.2633(9)	0.1579(6)	0.14(1)
C(115)	0.1174(7)	−0.0023(5)	0.9543(6)	0.100(7)	C(215)	0.1435(7)	0.4381(6)	0.3565(6)	0.094(7)
C(116)	0.2318(6)	0.1243(6)	1.0036(6)	0.096(6)	C(216)	0.2978(8)	0.5145(5)	0.4370(6)	0.104(8)
C(117)	0.1915(7)	0.0609(6)	0.8658(6)	0.104(7)	C(217)	0.2558(8)	0.3824(6)	0.4977(6)	0.095(7)

[a] See Table 3.

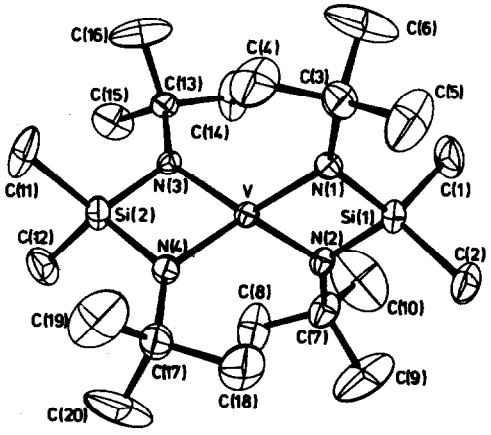

Fig. 2. A perspective drawing of $V[(N\text{-}t\text{-}Bu)_2SiMe_2]_2$ with 20% probability thermal ellipsoids and H atoms omitted.

numbering schemes are defined in Figures 1, 2, 3 and 4. SHELX-76 [21], ORTEP-II [22] and several local programs were used. Supplementary data are available [23].

Description of the crystal structures

$M[(N\text{-}t\text{-}Bu)_2SiMe_2]_2$

The hafnium derivative III is isomorphous with $Zr[(N\text{-}t\text{-}Bu)_2SiMe_2]_2$ [9] and the low-temperature modification of $Sn[(N\text{-}t\text{-}Bu)_2SiMe_2]_2$ [24], and even with $Li_4[(N\text{-}t\text{-}Bu)_2SiMe_2]_2$ [25] since the center of the Li_4 cluster coincides with the Hf atom of III. The crystallographic relationships between these structures are outlined in the deposited material [23]. On the other hand, the tetragonal modification of the vanadium derivative IV has not previously been observed for these spirocyclic derivatives.

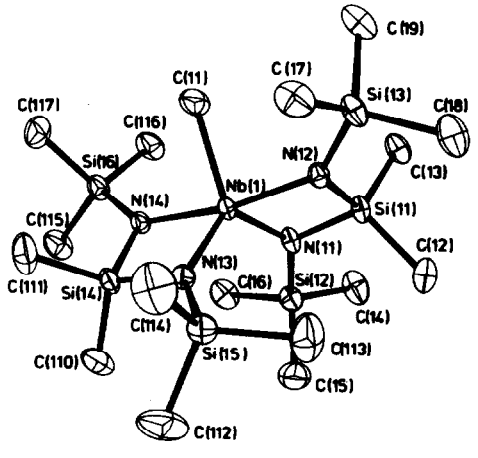

Fig. 3. A perspective drawing of molecule 1 of $MeNb[(NSiMe_3)_2SiMe_2]_2$ with 20% probability thermal ellipsoids and H atoms omitted.

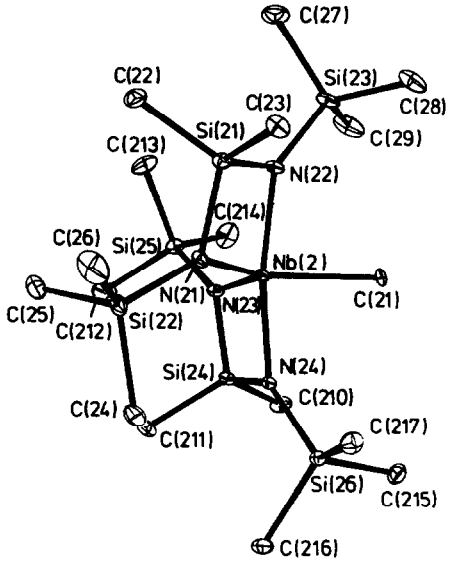

Fig. 4. A perspective drawing of molecule 2 of $MeNb[(NSiMe_3)_2SiMe_2]_2$ with 5% probability thermal ellipsoids and H atoms omitted.

The structures contain two nearly planar units (r.m.s. deviations of 0.018 Å in III

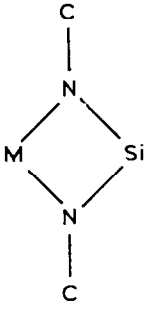

and 0.015 Å in IV) which are mutually orthogonal, the dihedral angles being 89.5(6) and 87.8(4)° for III and IV, respectively. In addition, the conformation of each t-BuN moiety is such as to form one small M–N–C–C torsion angle per group, the average values being 5(4)° in III and 9(8)° in IV, and the Si–M–Si backbones of these molecules are approximately linear (III: 176.6(1)°; IV: 178.7(1)°). Thus approximate $\bar{4}2m$ (D_{2d}) symmetry is found, in agreement with that reported for the analogous compounds with M = Ti, Zr [9] and Sn [24]. The crystallographic twofold axis that intersects the Hf atom of III lies perpendicular to the $\bar{4}$ axis of the molecular point group. Averaged distances and angles are listed in Table 6.

The planarity of the nitrogen valencies in these and numerous other metal amides might imply that the N atoms are three-electron donors; that is, that they form a covalent M–N σ bond and a dative N($p\pi$) → M(π) π bond; simple electron counting procedures would then imply that the metal atoms of III and IV achieve 16- and 17-electron configurations, respectively. However, this simple approach to electron counting is incorrect. With $\bar{4}2m$ symmetry, the N($p\pi$) orbitals transform

TABLE 6

SELECTED BOND DISTANCES (Å) AND ANGLES(°) [a] IN $M[(N\text{-}t\text{-}Bu)_2SiMe_2]_2$ (M = Hf, V)

	Hf	V
M–N	2.030(4)	1.853(5)
Si–N	1.751(8)	1.740(3)
Si–C	1.861(8)	1.872(4)
N–C	1.478(8)	1.465(8)
C–C	1.442(8)	1.495(3)
N–M–N [b]	78.8(3)	84.8(1)
N–M–N [c]	126.6(7)	123.1(7)
M–N–C	137.4(5)	136.8(2)
Si–N–C	129.4(4)	131.4(2)
M–N–Si	93.2(2)	91.8(1)
N–Si–N	94.8(3)	91.8(1)
C–Si–C	108.3(6)	106.9(3)
N–Si–C	113.3(6)	114.5(2)
N–C–C	110.8(6)	110.6(3)
C–C–C	108.1(7)	108.2(4)

[a] Chemically equivalent values have been averaged, standard deviations being the larger of $[\Sigma\sigma^2(l)]^{1/2}/n$ and $[\Sigma(l-\bar{l})^2/n(n-1)]^{1/2}$. [b] Endocyclic angle. [c] Exocyclic angle.

as $e + a_2 + b_1$. Since no metal orbital transforms as a_2, the four N atoms can donate no more than six electrons to the metal atoms by dative $N(p\pi) \rightarrow M(\pi)$ bonding. Therefore, only 14- and 15-electron configurations can be attained by the metal atoms of III and IV, respectively.

The mean Hf–N bond length in III, 2.030(4) Å, agrees well with that found in $Hf[N(SiMe_3)_2]_3Cl$, 2.04(1) [26]. No structure of an amide containing four-coordinate vanadium has been described previously; however, the V–N bonds in IV,

TABLE 7

SELECTED BOND DISTANCES (Å) AND ANGLES (°) [a] IN $MeNb[(NSiMe_3)_2SiMe_2]_2$

$Nb–N_e$ [b]	1.997(4)	Nb–C	2.218(9)
$Nb–N_a$	2.026(5)	$Si_r–N_e$	1.749(4)
$Si_e–C$	1.848(6)	$Si_r–N_a$	1.741(6)
$Si_a–C$	1.856(7)	$Si_e–N_e$	1.733(4)
$Si_r–C$	1.855(5)	$Si_a–N_a$	1.736(4)
$C–Nb–N_e$	121 (2)	$Nb–N_e–Si_r$	93.3(4)
$C–Nb–N_a$	85.0(2)	$Nb–N_a–Si_r$	92.4(3)
$N_e–Nb–N_e'$ [c]	118.9(3)	$N_e–Si_r–N_a$	94.8(2)
$N_a–Nb–N_a'$	169.2(3)	$N_e–Si_r–C$	112.8(2)
$N_a–Nb–N_e$	79.4(4)	$N_a–Si_r–C$	113.0(2)
$N_a–Nb–N_e'$	106 (1)	$N_e–Si_e–C$	110.6(3)
$Nb–N_e–Si_e$	137 (1)	$N_a–Si_a–C$	110.9(4)
$Nb–N_a–Si_a$	139.1(2)	$C–Si_e–C$	108.3(5)
$Si_r–N_e–Si_e$	126.8(5)	$C–Si_a–C$	108.0(4)
$Si_r–N_a–Si_a$	126.4(4)	$C–Si_r–C$	109.6(5)

[a] Individual values have been averaged assuming C_2 symmetry at the Nb atoms and equivalence of the groups of Si–C bonds. [b] N_e and Si_e refer to an equatorial N atom and its exocyclic substituent respectively, N_a and Si_a are corresponding atoms in axial position and Si_r is a ring Si atom. [c] A primed N atom is not in the four-membered ring of the unprimed N atom.

TABLE 8

METAL–NITROGEN BOND LENGTHS (Å) IN SPIROCYCLIC COMPOUNDS

Compound	M [a]–N	Δ [b]	Ref.
$Ti[(N\text{-}t\text{-}Bu)_2SiMe_2]_2$	1.890(4)	0.566(4)	9
$Ti[(NMeSiMe_2)_2]_2$	1.905(5)	0.581(5)	33
$Ti[(NSiMe_3)_2SiPh_2]_2$	1.918(2)	0.594(2)	32
$Zr[(N\text{-}t\text{-}Bu)_2SiMe_2]_2$	2.053(2)	0.599(2)	9
$Hf[(N\text{-}t\text{-}Bu)_2SiMe_2]_2$	2.030(4)	0.588(4)	[c]
$Sn[(N\text{-}t\text{-}Bu)_2SiMe_2]_2$	2.034(8)	0.635(8)	24
$V[(N\text{-}t\text{-}Bu)_2SiMe_2]_2$	1.853(5)	0.629(5)	[c]
$MeNb[(NSiMe_3)_2SiMe_2]_2$	2.012(6)	0.670(6)	[c]

[a] M is the spirocyclic center. [b] Difference between the M–N bond length and Pauling's [31] single-bond metallic radius for M. [c] This work.

1.853(5) Å, are comparable to those formed by μ-NPh ligands, 1.89(2) Å, in a trinuclear cluster containing pentavalent V atoms [27].

The N–C bonds are not perpendicular to the M–Si vectors but are tilted by 8.0(5)° in III and 4.4(2)° in IV further away from the spirocyclic centers. These tilts T are easily calculated from the expression

$$T = (M\text{–}N\text{–}C) - (N\text{–}M\text{–}N)/2 - 90°$$

Values thus calculated for other $M[(N\text{-}t\text{-}Bu)_2SiMe_2]_2$ compounds are 5.7(2), 7.5(2) and 3.3(4)° for M = Ti, Zr and Sn, respectively. If these tilts were the result of attempts to relieve steric crowding in the middle of the molecules [24], then T should decrease as the M–N distance increases (Table 8), but the data reveal no such behavior. It is possible that electronic factors influence these angles, since T tends to decrease as the electronegativity of M increases.

The shortness of the C–C bond lengths in III and IV appears to be an artifact of the large torsional amplitudes exhibited by the t-Bu groups about their N–C bonds. The TLS [28] rigid-body-motion model fits the NCC_3 fragments adequately, and the C–C bond lengths corrected for librational shortening are much more acceptable (III: 1.55(2) Å; IV: 1.58(2) Å).

$MeNb[(NSiMe_3)_2SiMe_2]_2$

The two crystallographically independent molecules of VIII possess very similar spirocyclic structures; indeed, the coordinates of the second molecule may be roughly estimated from those of the first by the pseudosymmetry operation $z - x - 0.5$, $0.5 - y$, $z - 0.5$. (The crystal structure can, in fact, be described fairly well in terms of a centered orthorhombic cells, but careful examination of Weissenberg photographs, the monoclinic cell contstants, and the final coordinates confirmed that the symmetry is no higher than monoclinic.) Each NbN_2Si four-membered ring is planar (r.m.s. deviations < 0.02 Å), but in contrast to the orthogonal disposition of the corresponding rings in III and IV, dihedral angles of 65.6(8) and 64.6(8)° are formed by the normals to these rings in the two molecules of VIII. The smaller values for these angles in VIII reflect the higher coordination number of the central metal atom. Indeed these angles are close to the 60° value required for the dihedral angle between planes defined by alternate pairs of axial and equatorial bonds of a trigonal bipyramid.

An equatorial Nb–C bond completes each Nb coordination sphere. This bond

coincides with an effective twofold axis of the molecule, the most serious violation of which is the 6(1)° average difference in the two equatorial C–Nb–N bond angles, and this symmetry has been assumed in deriving the average bond distances and angles referred to below. The nitrogen atoms in axial (N(12), N(14), N(22) and N(24)) and equatorial positions are denoted by N_a and N_e, respectively, and their corresponding exocyclic substituents are labelled Si_a and Si_e (Table 7).

The N_e–Nb–N_e' bond angle of 118.9(3)° is close to the ideal value for a trigonal bipyramid. However, the angles N_a–Nb–N_a', 169.2(3)°, and C–Nb–N_a, 85.0(2)°, are somewhat smaller than the relevant trigonal-bipyramidal values of 180 and 90°. Further opening of these angles will shorten the interligand $Si_aMe_3 \cdots Si_eMe_3$ contacts, and these are already so close that there are distances of less than 2.5 Å between one or more pairs of idealized H atom positions in each case. The repulsive nature of these contacts is revealed by the fact that the Si_a and Si_e atoms are displaced by as much as 0.565(4) Å from the planes of the associated NbN_2Si four-membered rings in directions which relieve the overcrowding. Normally these atoms would be inplane substituents, as are the quaternary C atoms of III and IV. As far as alternative structures are concerned, interligand steric repulsions would certainly be much greater if each metal–amide bond of VIII were located in the basal plane of a square-pyramidal structure like that reported for t-BuTa$(NMe_2)_4$ [29].

The Nb–N_a bonds, 2.026(5) Å, are significantly longer than the Nb–N_e linkages, 1.997(4) Å. These values may be compared to the corresponding axial and basal bond lengths reported for the square-pyramidal structures of Nb$(NMe_2)_5$ (1.98 (2), 2.04(1) Å) and Nb$(NC_5H_{10})_5$ (1.99(1), 2.05(1) Å) [30]. Although the covalent radius of nitrogen is only 0.07 Å less than that of carbon, the Nb–N_e distance is 0.22(1) Å shorter than the Nb–C bond. Similar differences in M–N and M–C bond lengths in $(PhCH_2)_2Ti[N(SiMe_2NMe)_2SiMe_2]_2$ [19] and t-BuTa$(NMe_2)_4$ [29] have been rationalized in terms of $N(\pi) \rightarrow M(\pi)$ bonding.

For a series of closely related metal amide structures the variation in the M–N distances might be related to variations in the single-bond metallic radii [31]. These radii have been subtracted from the corresponding M–N distances in a variety of spirocyclic metal amides, and the differences Δ are listed in Table 8. Since all of the values of Δ are less than the covalent radius of nitrogen (0.70 Å), strong M–N bonding can be assumed in each case. For the t-Bu substituted derivatives with M = Ti, Zr and Hf, the significantly smaller Δ for M = Ti may indicate somewhat stronger M–N bonding for that compound. That Δ for M = Nb is 0.041(8) Å larger than that for M = V, may be a $SiMe_3$/t-Bu substitution effect, since the Ti–N bonds in $Ti[(NSiMe_3)_2SiPh_2]_2$ [32] are 0.028(5) Å longer than those in $Ti[(N\text{-}t\text{-}Bu)_2SiMe_2]_2$ [9]. Why the values of Δ for M = Ti, Zr and Hf are all smaller than those for M = V and Nb remains a matter of conjecture. Conceivably the M–N distances in the latter two compounds are lengthened by interaction between electrons in the valence shells of the metals but not associated with M–N bonds. Finally, the fact that Δ for M = Sn is similar to that for M = V emphasizes the potential for strong M–N bonding by elements other than the transition metals.

Experimental

Synthesis

The dilithiated amines I and II were prepared from the respective amines [16,17] with BuLi in n-hexane and used in solution.

TABLE 9

ELEMENTAL ANALYSES

Compound	Formula	Analyses (Found (calcd.)(%))				
		C	H	Cl	N	metal
III	$C_{20}H_{48}HfN_4Si_2$				9.3 (9.67)	30.2 (30.81)
IV	$C_{20}H_{48}N_4Si_2V$				12.3 (12.40)	11.2 (11.28)
V	$C_{16}H_{48}N_4Si_6V$				10.4 (10.86)	9.6 (9.87)
VI	$C_{16}H_{48}ClN_4NbSi_6$	32.8 (32.38)	8.5 (8.15)	5.6 (5.97)	9.2 (9.44)	15.8 (15.65)
VII	$C_{16}H_{48}ClN_4Si_6Ta$			5.3 (5.21)	7.9 (8.23)	26.9 (26.55)
VIII	$C_{17}H_{51}N_4NbSi_6$				9.6 (9.78)	16.2 (16.21)
IX	$C_{17}H_{51}N_4Si_6Ta$				8.5 (8.47)	27.5 (27.37)

1,3,5,7-Tetra-t-butyl-2,2,6,6-tetramethyl-1,3,5,7-tetraaza-2,6-disila-4-hafnaspiro [3.3]heptane (III). A solution of 40 mmol I in 150 ml petroleum ether was added to a suspension of 6.4 g (20 mmol) $HfCl_4$ in a mixture of 150 ml toluene and 50 ml Et_2O. The mixture was stirred for 18 h then briefly heated under reflux. The LiCl was filtered off, the solvent removed in vacuo, and the residue sublimed in vacuo, yield 44%. Elemental analyses are given in Table 9.

Raman: 121vw, 149vw, 179s, 203vs, 236s, 266s, 344s, 362w, 425vw, 538vs, 623w, 651s, 679vw, 717vw, 774w, 784s, 848w, 913m, 1038w, 1094w, 1225m, 1415vw, 1455w, 1475m.

IR: 359m, 386w, 420w, 498s, 512w, 551m, 622vw, 649s, 671m, 722w, 755vs, 776vs, 790sh, 819s, 838vs, 919vw, 974m, 1011sh, 1043vs, 1203vs, 1238w, 1246vs.

MS: $m/e = 580$ $(M)^+$, 4%; 565 $(M - Me)^+$, 75%; 200, 15%; 187, 82%; 130, 75%; 114, 100%; 74, 53%; 73, 58%; 58, 35%; 57, 22%.

1,3,5,7-Tetra-t-butyl-2,2,6,6-tetramethyl-1,3,5,7-tetraaza-2,6-disila-4-vanadaspiro-[3.3]heptane (IV). This was made analogously from I and VCl_4 in petroleum ether; yield 38%.

Raman: 135w, 184vs, 245w, 271s, 347s, 539m, 573w, 657m, 796s, 830vw, 863w, 914vw, 1055m, 1073w, 1235m.

IR: 411sh, 419m, 502m, 546vw, 577vw, 660s, 722w, 750vs, 769s, 798m, 819m, 838vs, 891vw, 920vw, 973m, 1030w, 1051vs, 1075vw, 1207vs, 1246s.

MS: $m/e = 451$ $(M)^+$, 13%; 436 $(M - Me)^+$, 6%; 379, 4%; 363, 7%; 251, 5%; 187, 18%; 185, 4%; 130, 17%; 114, 22%; 74, 10%; 73, 12%; 58, 100%; 57, 28%.

1,3,5,7-Tetrakis(trimethylsilyl)-2,2,6,6-tetramethyl-1,3,5,7-tetraaza-2,6-disila-4-vanada-spiro[3.3]heptane (V). This was made analogously from II and VCl_4; yield 53%.

IR: 403s, 469s, 608vs, 646vs, 686w, 709vs, 723m, 767vs, 778vw, 790vw, 845vs, 996vs, 1249vs.

MS: $m/e = 515$ $(M)^+$, 100%; 500 $(M - Me)^+$, 3%; 484, 5%; 468, 20%; 421, 10%; 405, 10%; 219, 95%; 203, 36%; 187, 6%; 146, 15%; 73, 56%.

1,3,5,7-Tetrakis(trimethylsilyl)-4-chloro-2,2,6,6-tetramethyl-1,3,5,7-tetraaza-2,6-disila-4-nioba-spiro[3.3]heptane (VI). This was made analogously from II and $NbCl_5$ in Et_2O; yield 49%.
Raman: 113w, 164vs, 189s, 309s, 362vs, 383s, 419vw, 435m, 628s, 642s, 681s, 741m, 788s, 845m, 944m, 981vw, 1029vs, 1145vw, 1249m.
IR: 401w, 420m, 434vw, 583m, 620s, 646vs, 687w, 716vs, 771vs, 781sh, 846vs, 950vs, 985vw, 1252vs.
MS: $m/e = 577$ $(M - Me)^+$, 2%; 295, 12%; 219, 80%; 203, 31%; 146, 100%; 131, 66%; 130, 82%; 100, 22%; 93, 22%; 73, 82%.

1,3,5,7-Tetrakis(trimethylsilyl)-4-chloro-2,2,6,6-tetramethyl-1,3,5,7-tetraaza-2,6-disila-4-tantala-spiro[3.3]heptane (VII). This was made analogously from II and $TaCl_5$ in Et_2O; yield 23%.
Raman: 111sh, 165vs, 190s, 236vw, 316m, 363s, 382m, 406w, 441vw, 627s, 645vs, 682s, 747vw, 778w, 788w, 845m, 945w, 1046m, 1248m.
IR: 397m, 440m, 575sh, 602w, 625m, 644s, 685w, 719vs, 778vs, 848vs, 955vs, 995vw, 1252vs.
MS: $m/e = 665$ $(M - Me)^+$, 23%; 219, 55%; 203, 30%; 146, 58%; 130, 46%; 93, 22%; 73, 100%.

1,3,5,7-Tetrakis(trimethylsilyl)-2,2,4,6,6-pentamethyl-1,3,5,7-tetraaza-2,6-disila-4-nioba-spiro[3.3]heptane (VIII). A solution of 2 ml MeLi (1.8 *M* in Et_2O) was added to a solution of 2.13 g (3.6 mmol) VI in 10 ml Et_2O and the mixture was stirred for 3 h. The solvent was removed in vacuo and the residue extracted with 10 ml petroleum ether. The extract was concentrated to 2 ml and cooled to $-25°C$ to give yellow crystals; yield 82%.
Raman: 163vs, 179s, 232vw, 306w, 351vs, 383s, 430w, 482m, 627s, 643vs, 684s, 744vw, 788s, 847m, 956m, 996vw, 1036s, 1151m.
IR: 405w, 419m, 435sh, 485vw, 505w, 591s, 622vw, 644s, 685m, 715vs, 772vs, 791sh, 848vs, 885sh, 955vs, 990sh, 1252vs.
MS: $m/e = 557$ $(M - Me)^+$, 24%; 219, 100%; 203, 49%; 131, 67%; 130, 48%; 73, 44%.

1,3,5,7-Tetrakis(trimethylsilyl)-2,2,4,6,6-pentamethyl-1,3,5,7-tetraaza-2,6-disila-4-tantala-spiro[3.3]heptane (IX). This was made by the procedure used for VIII, but starting from VII; yield 65%.
Raman: 114w, 173vs, 193vs, 235w, 311w, 353s, 382m, 408w, 435vw, 489m, 628s, 644vs, 682s, 750vw, 778m, 790w, 845m, 953w, 1043m, 1171m, 1247m.
IR: 395m, 438m, 495w, 569vw, 603m, 626vw, 641s, 688m, 722s, 778vs, 796sh, 849vs, 885sh, 955vs, 996vw, 1252vs.
MS: $m/e = 645$ $(M - Me)^+$, 16%; 615, 2%; 219, 100%; 203, 47%; 131, 69%; 130, 55%; 73, 40%.

Spectra were obtained as described in ref. 11. The cyclic voltammetry measurements were performed with a Metrohm Polarecord 626 instrument equipped with a E 612 VA scanner.

Acknowledgement

We thank Prof. Dr. Krüger of the Max-Planck-Institut für Kohlenforschung for recording the X-ray data on IV. Support by the Fonds der Chemie and by Bayer AG through a gift of chemicals is gratefully acknowledged.

References

1 M.F. Lappert, P.P. Power, A.R. Sanger and R.C. Srivastava, Metal and Metalloid Amides, Wiley Chichester, 1980.
2 R.A. Andersen, Inorg. Chem., 18 (1979) 1724.
3 R.A. Andersen, Inorg. Chem., 18 (1979) 3622.
4 H. Bürger and K. Wiegel, Z. Anorg. Allg. Chem., 419 (1976) 157.
5 H. Bürger and K. Wiegel, Z. Anorg. Allg. Chem., 426 (1976) 301.
6 H. Bürger, K. Wiegel, U. Thewalt and D. Schomburg, J. Organomet. Chem., 87 (1975) 301.
7 H. Schlingmann and U. Wannagat, Z. Anorg. Allg. Chem., 419 (1976) 115.
8 H. Bürger and D. Beiersdorf, Z. Anorg. Allg. Chem., 459 (1979) 111.
9 D.J. Brauer, H. Bürger, E. Essig and W. Geschwandtner, J. Organomet. Chem., 190 (1980) 343.
10 K. Wiegel and H. Bürger, J. Organomet. Chem., 129 (1977) 309.
11 H. Bürger, W. Geschwandtner and G.R. Liewald, J. Organomet. Chem., 259 (1983) 145.
12 R.A. Andersen, Inorg. Chem., 18 (1979) 2928.
13 D.F. Evans, J. Chem. Soc., (1959) 2003.
14 H.W. Turner, R.A. Andersen, A. Zalkin and D.H. Templeton, Inorg. Chem., 18 (1979) 1221.
15 E.C. Alyea and D.C. Bradley, J. Chem. Soc., A, (1969) 2330.
16 W. Fink, Helv. Chim. Acta, 47 (1964) 498.
17 U. Wannagat and H. Niederprüm, Z. Anorg. Allg. Chem., 308 (1961) 337.
18 D.J. Brauer, H. Bürger, G.R. Liewald and J. Wilke, J. Organomet. Chem., 287 (1985) 305.
19 D.J. Brauer, H. Bürger and K. Wiegel, J. Organomet. Chem., 150 (1978) 215.
20 International Tables for X-ray Crystallography, Vol. IV, Tables 2.2 B and 2.3.1, The Kynoch Press, Birmingham (1974).
21 G.M. Sheldrick, SHELX-76, Program for crystal structure determination, University of Cambridge, England 1976.
22 C.K. Johnson, ORTEP-II, Report ORNL-5138, Oak Ridge National Laboratory, Tennessee 1976.
23 F_o, F_c lists, tables of hydrogen coordinates and anisotropic thermal parameters may be obtained from Fachinformationszentrum Energie Physik Mathematik, D-7514 Eggenstein-Leopoldshafen 2, by quoting the deposit number CSD 52003, the names of the authors and the literature reference.
24 M. Veith, Z. Anorg. Allg. Chem., 446 (1978) 227.
25 D.J. Brauer, H. Bürger and G.R. Liewald, J. Organomet. Chem., 308 (1986) 119.
26 C. Airoldi, D.C. Bradley, H. Chudzynska, M.B. Hursthouse, K.M.A. Malik and P.R. Raithby, J. Chem. Soc., Dalton Trans., (1980) 2010.
27 D.C. Bradley, M.B. Hursthouse, A.N. de M. Jelfs and R.L. Short, Polyhedron, 2 (1983) 849.
28 V. Schomaker and K.N. Trueblood, Acta Crystallogr., B 24 (1968) 63.
29 M.H. Chisholm, L.-S. Tan and J.C. Huffman, J. Amer. Chem. Soc., 104 (1982) 4879.
30 C. Heath and M.B. Hursthouse, J. Chem. Soc., Chem. Commun., (1971) 143.
31 L. Pauling, The Nature of the Chemical Bond, Cornell (1960).
32 W.D. Beiersdorf, D.J. Brauer and H. Bürger, Z. Anorg. Allg. Chem., 475 (1981) 56.
33 H. Bürger, K. Wiegel, U. Thewalt and D. Schomburg, J. Organomet. Chem., 87 (1975) 301.